Project no. TIP5-CT-2006-031415

INNOTRACK

Integrated Project (IP)

Thematic Priority 6: Sustainable Development, Global Change and Ecosystems

D4.3.2 Characterisation of Microstructural Changes in Surface & Sub-surface Layers of Rails with Traffic

Due date of deliverable: 2007-08-31

Actual submission date: 2007-10-11

Start date of project: 1 September 2006 Duration: 36 months

Organisation name of lead contractor for this deliverable: Corus Group plc

Revision draft 3

Project co-funded by the European Commission within the Sixth Framework Programme (2002-2006)		
Dissemination Level		
PU	Public	X
PP	Restricted to other programme participants (including the Commission Services)	
RE	Restricted to a group specified by the consortium (including the Commission Services)	
CO	Confidential, only for members of the consortium (including the Commission Services)	

Table of Contents

Glossary

EBSD	Electron back scatter diffraction
RCF	Rolling contact fatigue
SCL	Surface crack length, measured in mm
POI	Position of initiation, measured as the distance in mm from the active side of head
SoH	Side of Head
SEM	Scanning Electron Microscope

1. Executive Summary

Rolling Contact Fatigue (RCF) of rails, whether manifested as head checking, gauge corner cracking or squats, continues to be one of the key rail degradation mechanisms reducing the life span of rails with a significant adverse impact on the Life Cycle Cost of the track infrastructure. Not surprisingly, this issue and, more generally, the rail-wheel interface and its implications for track maintenance have been the most prominent topic of railway research. However, although plastic deformation and resulting work hardening of the surface and sub-surface layers of the rail are universally acknowledged, a quantitative assessment of this microstructural damage and property change has been restricted to measurement of micro hardness.

The work reported in this document has provided an alternative way of assessing the misorientation of grains as a result of the passage of traffic through the use of Electron Back Scatter Diffraction techniques. Although based on a relatively small number of samples, the work has demonstrated that the thickness of the damaged layer reduces with increasing hardness of the rail. Implications of this finding on the magnitude of metal removal during grinding have been briefly discussed and this document is expected to serve as a discussion document to formulate a programme of work to answer the questions and hypothesis presented.

The work has also demonstrated that Scanning Electron Microscopy provides a useful way of examining RCF affected running surfaces and has shown that RCF cracks are a consequence of plastic deformation of very thin layers of material to create ledges. It has been found that replicas can be used to study this surface deformation phenomenon and could be used to look at both RCF-free and RCF affected track.

In view of the very encouraging results, the scope of the original work programme and the deliverable 4.3.2 has been significantly increased to examine a larger number of samples and consequently, this document should be treated as an interim deliverable with the final document to be delivered later.

2. Introduction

Rolling Contact Fatigue (RCF) of rails, whether manifested as head checking, gauge corner cracking or squats, continues to be one of the key rail degradation mechanisms reducing the life span of rails with a significant adverse impact on the Life Cycle Cost of the track infrastructure. Not surprisingly, this issue and, more generally, the rail-wheel interface and its implications for track maintenance have been the most prominent topic of railway research. However, although plastic deformation and resulting work hardening of the surface and sub-surface layers of the rail are universally acknowledged, a quantitative assessment of this microstructural damage and property change has been restricted to measurement of micro hardness.

The programme of work reported in this document is a novel application of micro structural analysis techniques developed and successfully employed in other areas of metal research. It should also be emphasized that as the usefulness of the proposed technique became apparent from the study of the early samples from a single grade of rail steel, the scope of the work has been significantly enlarged to include some premium rail grades. Hence, the current report should be treated as an interim and a final report detailing the implications of the extent of the damaged layer on the optimum selection of rail grades and their maintenance will be produced by end August 2008.

3. Project Objectives and Scope

The primary objective of the work undertaken relates to Project Deliverable 4.3.2 and involves the “Characterisation of microstructural changes in surface and sub-surface layers with traffic”. In this context, the intention was to employ novel examination techniques to characterise the microstructural changes that occur at the contact surface and sub-surface into the rail with the passage of traffic.

In view of the application of novel techniques, the project scope was initially restricted to study of samples of Grade 220 rail taken out of UK track. However, encouraged by the early results, the project scope was enlarged to include a matrix of rail grades and traffic conditions.

3.1 Matrix of Samples Examined

The matrix of samples examined is presented in Table 1 below. Although an ideal experimental programme would require a full factorial design of the key variables, the chosen matrix of samples is considered to provide a reasonably wide coverage to enable meaningful conclusions to be drawn:

1. The full range of RCF condition from Clear to Severe crack categories
2. The full range of rail hardness from 220 to 400 HB
3. Two track forms: Ballasted and slab track
4. Four Railway networks: DB (Germany), Heathrow Express (HEx, UK), NR (UK), & ProRail (Netherlands)

Table 1 Matrix of Samples Examined

Rail Steel Grade	IM Network	Track Form	RCF Status				
			RCF-Free	Light	Moderate	Heavy	Severe
220 NR		Ballasted	✓	✓	✓	✓	✓
260	DB	Ballasted		✓	✓	✓	✓
	Other UK	Slabtrack				✓	
350HT NR		Ballasted		✓			✓
400 HB+	ProRail	Ballasted					✓

Brief details of the in-track service history of the above samples are presented in Table 2 below. The differences in track radius, cant, traffic carried in the samples examined are apparent and their potential effect on the observed microstructural changes is noted and will be appropriately considered in the discussion of results in a later section.

Table 2 In Track Characteristics of Samples Examined

Rail Grade	Rail Source/ Sample No.	Location	RCF* Category	Rail Year	Rail Section	Curve Radius (m)	Cant	Total Traffic (MGT)
220	NR/1	Newton Hall	RCF Free	1989	56 E1	1100	125	144.2
220	NR/2	Lamington	Light	1983	56 E1	1400	110	114.6
220	NR/3	Lamington	Moderate	1983	56 E1	1400	110	114.6
220	NR/4	Lamington	Heavy	1983	56 E1	1400	110	114.6
220	NR/5	Harringay	Severe	1964	56 E1	960	138	615.7
260	DB/6	Offenbach	Light	1994	54 E3	1200		200
260	DB/7	Offenbach	Moderate	1994	54 E3	1200		200
260	DB/8	Offenbach	Heavy	1994	54 E3	1200		200
260	DB/9	Offenbach	Severe	1994	54 E3	1200		200
260	HEx/10	UP 22.475Km	Severe	1996	UIC 54	1400		118.2
350HT	NR/11	Southside	Light	1992	56 E1	800	140	113.5
350HT	NR/12	Hatfield	Severe	1995	56 E1	1500	145	78.2
400+ HB	ProRail/ 13	Bunnik	Heavy	2000	54 E1	2275		~100

* Network Rail Rolling Contact Fatigue In Rails

3.2 Proposed Assessment Techniques

A comprehensive programme of assessment of the samples has been included in the extended scope of the project and includes:

1. Measurement of rail profiles: MiniProf measurements to be undertaken to establish magnitude of vertical, gauge corner, and side wear
2. Visual characterisation of RCF cracks: Measurement of Surface Crack Length, position of initiation on railhead, and vertical depth of RCF cracks.
3. High resolution Scanning Electron Microscopy: Assessment of RCF crack appearance on surface.
4. Electron Back Scatter Diffraction Analysis: This is a technique that uses the Scanning Electron Microscope (SEM) to obtain information about the crystallographic structure of the material. When electrons strike a crystalline sample, they are diffracted and form a pattern that is characteristic of the structure of the material. Information that can be obtained from the diffraction pattern includes grain misorientation, grain boundary orientation and texture. Notably, the quality of the pattern and range of orientations within grains can provide an indication of the deformation and the strain accumulated within the grains from the passage of wheels.

4. Results and Discussions

4.1 Comparison of Rail Profiles

Although the current programme is focussed on microstructural changes, the assessment of wear has been undertaken a s it is likely to have an influen ce on observed mi crostructural deformation. Miniprof profi le measurements of selected samples are shown in Figure 1 below and the data for vertical, gauge corner, and side wear is summarised in Table 3.

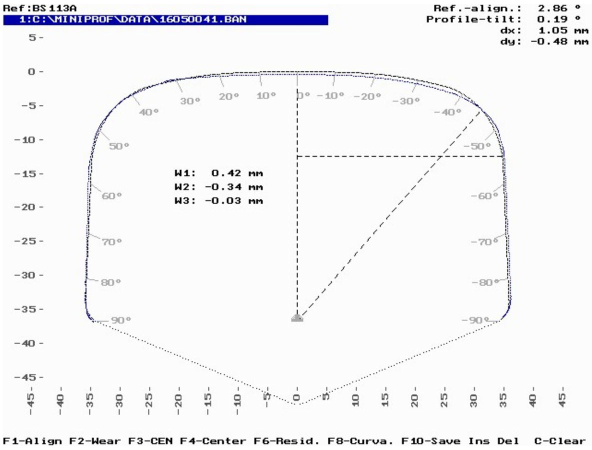

Figure 1a S1 (Newton Hall NR); Grade 220, 144 MGT; RCF Free

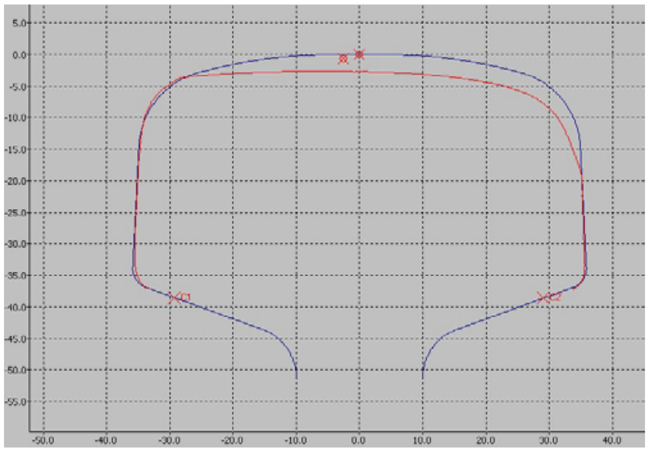

Figure 1b S2 (Lamington NR); Grade 220, 110 MGT; Light RCF

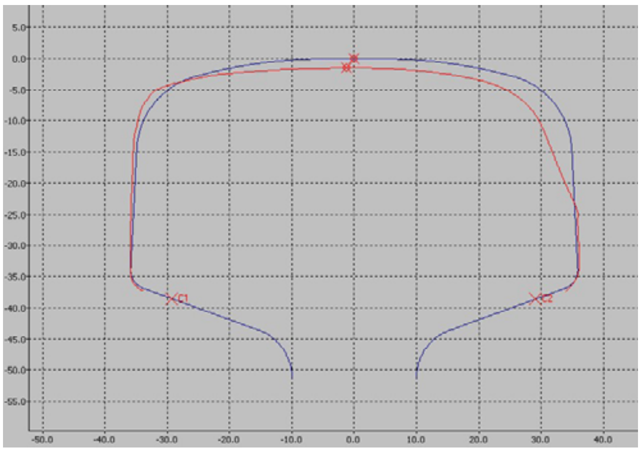

Figure 1c S3 (Lamington NR); Grade 220, 110 MGT; Moderate RCF

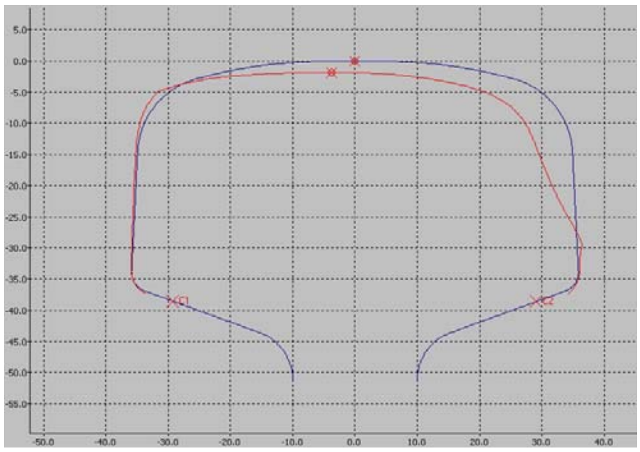

Figure 1d S4 (Lamington NR); Grade 220, 110 MGT; Heavy RCF

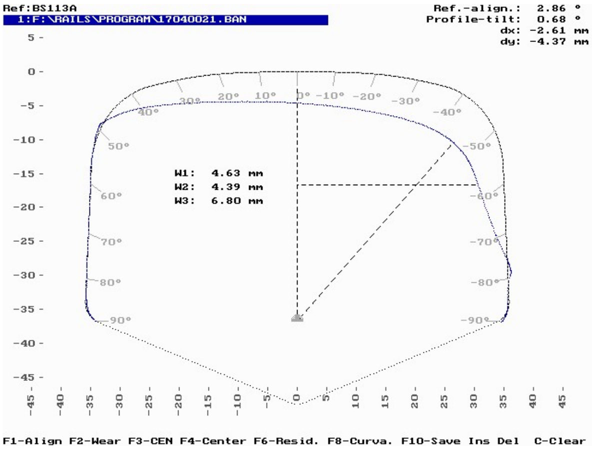

Figure 1e S5 (Harringay NR); Grade 220, 616 MGT; Severe RCF

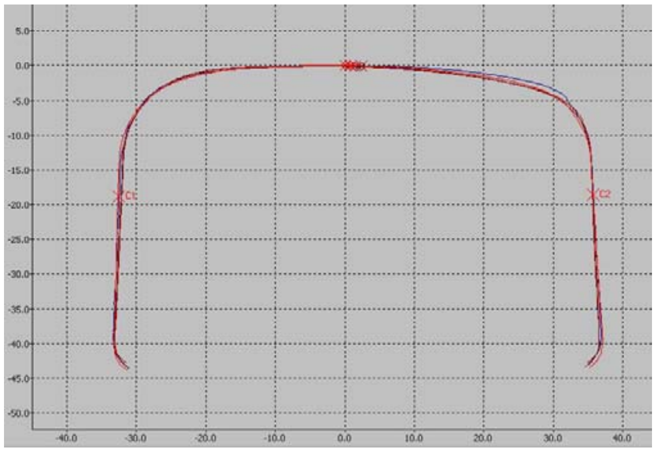

Figure 1f S6-9; Grade 260 (DB), 200 MGT; Light, Moderate, Heavy, Severe RCF

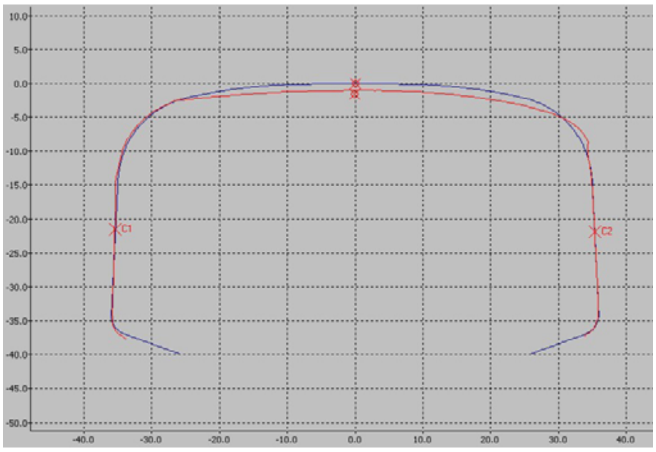

Figure 1g S10; Grade 260 (HEx), 118 MGT; Heavy RCF

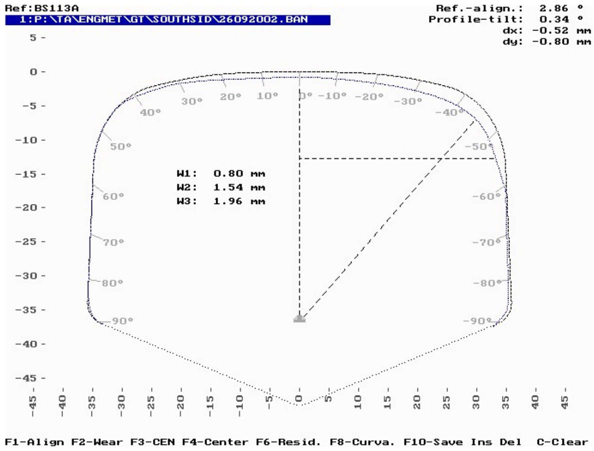

Figure 1h S11; Grade 350HT (South Side, NR), 114 MGT; Light RCF

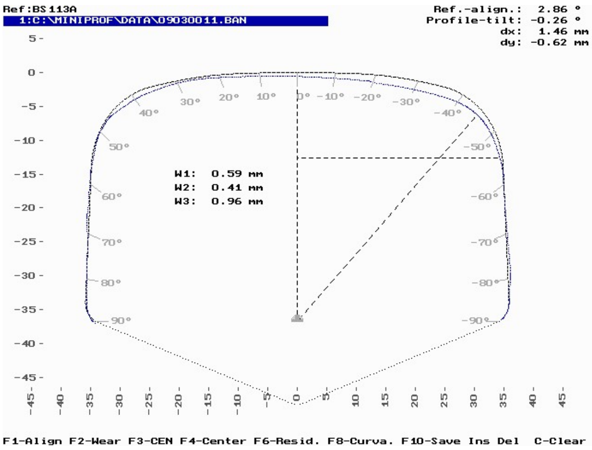

Figure 1i S12; Grade 350HT (Hatfield, NR), 78 MGT; Severe RCF

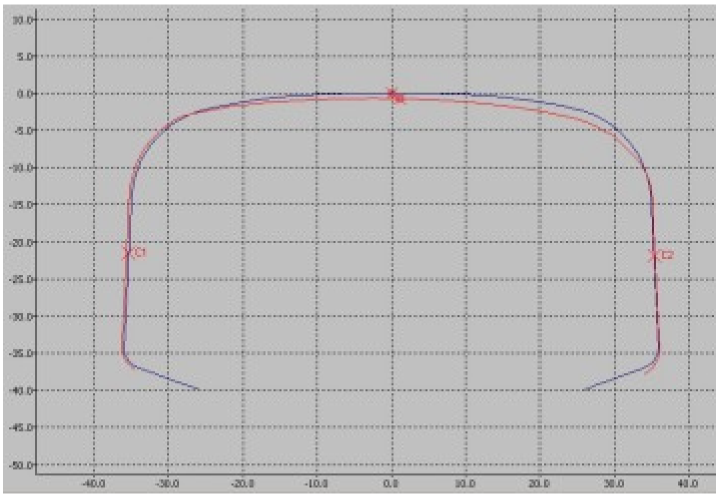

Figure 1j S13; Grade 400HB (Bunnik, ProRail), ~100 MGT; Severe RCF

Figure 1 Rail Profiles of Samples Examined

The key wear measurements of the samples examined are summarised in Table 3 below.

Table 3 Wear Measurements

Rail Grade	Rail Source/ Sample No.	Curve Radius (m)	Traffic (MGT)	Rail Section	Wear			RCF
					Vertical W1, mm	Side, W2, mm	Gauge, W3, mm	Category
220	NR/1	1100	144.2	56 E1	0.42	-	-	RCF Free
220	NR/2	1400	114.6	56 E1	2.73 2.04 2.28			Light
220	NR/3	1400	114.6	56 E1	1.51 3.92 3.72			Moderate
220	NR/4	1400	114.6	56 E1	1.85 6.15 5.76			Heavy
220	NR/5	960	615.7	56 E1	4.63 4.39 6.80			Severe
260 DB/6		1200	200	54 E3	0.84	0.07	-	Light
260 DB/7		1200	200	54 E3	1.03	-	0.64	Moderate
260 DB/8		1200	200	54 E3	1.18	-	0.51	Heavy
260	DB/9	1200	200	54 E3	0.49 0.13 0.34			Severe
260 HEx/10		1400	118.2	UIC 54	1.01	0.07	-0.88	Severe
350HT	NR/11	800	113.5	56 E1	0.80 1.54 1.96			Light
350HT	NR/12	1500	78.2	56 E1	0.59 0.41 0.96			Severe
400+ HB	ProRail/13	2275	~100	54 E1	0.70	-	0.959	Heavy

The following salient points can be gleaned from the measured profiles:

1. Although Sample 1 from Newton Hall is supposedly from a 1100m radius curve and has experienced ~144 M GT of traffic, the re i s vi rtually no gauge co rner or side wear and little verti cal wea r. Consequently, it is likely that the sample is from the transition into the curve.
2. All three La mington sa mples a re from within a short distance wi thin the cu rve, the observ ed side wear suggests eithe r varying flange contact o r v ariable a pplication of lub ricant. Ho wever, the difference is smaller in the case of verti cal wear or the wear at the point of RCF initiation. It is worth noting the increase in SCL of RCF cracks with increasing magnitude of gauge corner and side wear. This is probably an indication of crack growth through plastic deformation of the crack surfaces.
3. Sample 5 fro m a 960m radius cu rve at Harring ay on the ECM L netwo rk of NR shows a seve re category RCF cracks despite high levels of wear. However, the rate of wear does not appear to be higher than in other samples.
4. The four Grade 260 samples from the DB network are also from within the same curve. The samples with mode rate and he avy RCF cracks sho w very similar mag nitudes of vertical (W1) and Gaug e Corner (W3) wear but no side wear. In contrast, the samples with light and severe RCF cracks show lower ve rtical (W1) an d Gauge Corner (W3) wear but have a small amount of side (W2) wear. The differences suggest that the sample s may either be from diffe rent pa rts of t he curve or f rom the transition and the body of the cu rve. The examinatio n of the micros tructures of these sa mples may provide the necessary explanation for the varying susceptibility to the development of RCF cracks.
5. Sample 10 from the Heat hrow Express network fa lls at the limit o f heavy RCF category and shows very little we ar but with a little plastic deformation j ust bel ow th e active g auge corn er. A gain, the magnitude of deformation of the micro structure may provide th e reason for the observed l engths of cracks.
6. The 350 HT grade sa mples from So uthside (80 0m radiu s) a nd Hatfield (1 500m ra dius) and the 400HB grad e sa mple f rom Bunni k, ProRail (227 5m radius) reveal rel atively low level s of we ar particularly si nce these samples appear to have been ground at some stage. However, the sample from South side ha s light RCF while th e other two, despite co ming from shallower curve s exhibit severe category RCF cracks.

4.2 Visual and Electron Microscopy of Running Surface

Three specific techniques have been employed to characterise the surface appearance and the depth of RCF cracks:

1. **Visual Inspection:** This involved highlighting of the cracks using Magnetic Particle Inspection (MPI) technique to facilitate the measurement of the Surface Crack Length (SCL) and the Position of Initiation (POI). Previous destructive examination of a large number of RCF affected samples has established that the position of initiation is the furthest point of the crack from the active gauge face as indicated in the example diagram in Figure 2. Previous work, involving sectioning has been used to establish position of RCF initiation.

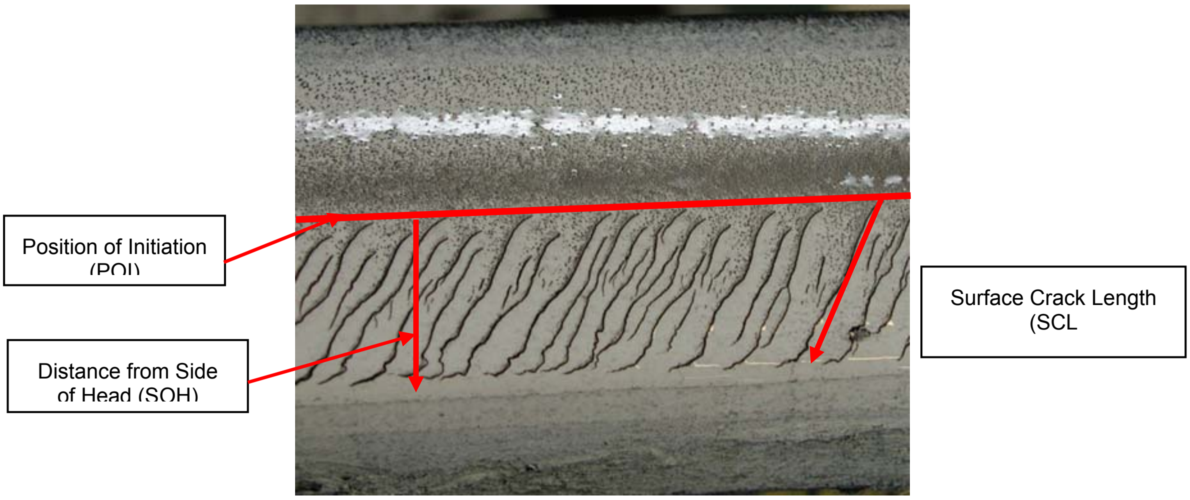

Figure 2 Determining RCF Characteristics

2. **Determination of Depth of RCF Cracks:** A longitudinal section was taken along a line close to the position of initiation and then ground back to reveal the maximum depth of the RCF cracks. An example of the cracks revealed in the longitudinal section is shown in Figure 3. The measured values of SCL, POI, and vertical depth for the various samples are given in Table 4.

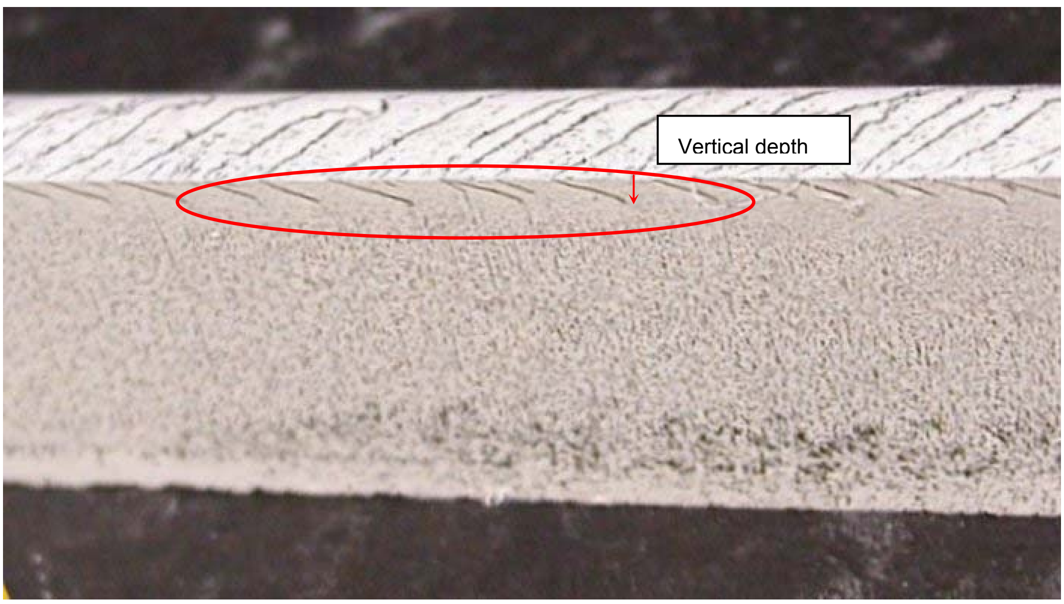

Figure 3 Determining the Maximum Vertical Depth of Cracks through Sectioning

Table 4 RCF Characteristics

Rail Grade	Rail Source/ Sample No.	Curve Radius (m)	Traffic (MGT)	Rail Section	Wear Vertical W1, mm	Wear Side, W2, mm	Wear Gauge, W3, mm	RCF Category	SCL (mm)	Depth* (mm)	POI (mm from SoH)
220	NR/1	1100	144.2	56 E1	0.42	-	-	RCF Free	0	0	0
220 NR/2		1400	114.6	56 E1	2.73	2.04	2.28	Light	7.6	2.0	25
220 NR/3		1400	114.6	56 E1	1.51	3.92	3.72	Moderate	13	3.5	25
220 NR/4		1400	114.6	56 E1	1.85	6.15	5.76	Heavy	23	5.5	25
220 NR/5		960	615.7	56 E1	4.63	4.39	6.80	Severe	35	9.0	28
260 DB/6		1200	200	54 E3	0.84	0.07	-	Light	13	2.0	17
260	DB/7	1200	200	54 E3	1.03 - 0.64			Moderate	19	3.0	25
260	DB/8	1200	200	54 E3	1.18 - 0.51			Heavy	28	5.0	28
260 DB/9		1200	200	54 E3	0.49	0.13	0.34	Severe	30	5.0	30
260 HEx/10		1400	118.2	UIC 54	1.01	0.07	-0.88	Severe	30	2.0	31
350HT NR/11		800	113.5	56 E1	0.80	1.54	1.96	Light	4	1.0	7
350HT NR/12		1500	78.2	56 E1	0.59	0.41	0.96	Severe	33	8.0	30
400+ HB	ProRail/13	2275	~100	54 E1	0.70	-	0.959	Heavy	23	6.0	20

* Measured vertical depth of RCF through sectioning

3. **<u>High Resolution Scanning Electron Microscopy:</u>** This technique has the advantage of a high depth of focus and hence can be used to examine how the surface layers of the rail have been deformed by the passage of traffic in both RCF- free and RCF affected rails. A knowledge of the magnitude of deformation of surface layers as a function of rail steel grade/hardness is necessary to provide an intelligent guideline for the selection of rail grades.

Photographs in the MPI enhanced condition and that as revealed by Scanning Electron Microscopy are shown in Figure 4 for a selection of samples used within this investigation.

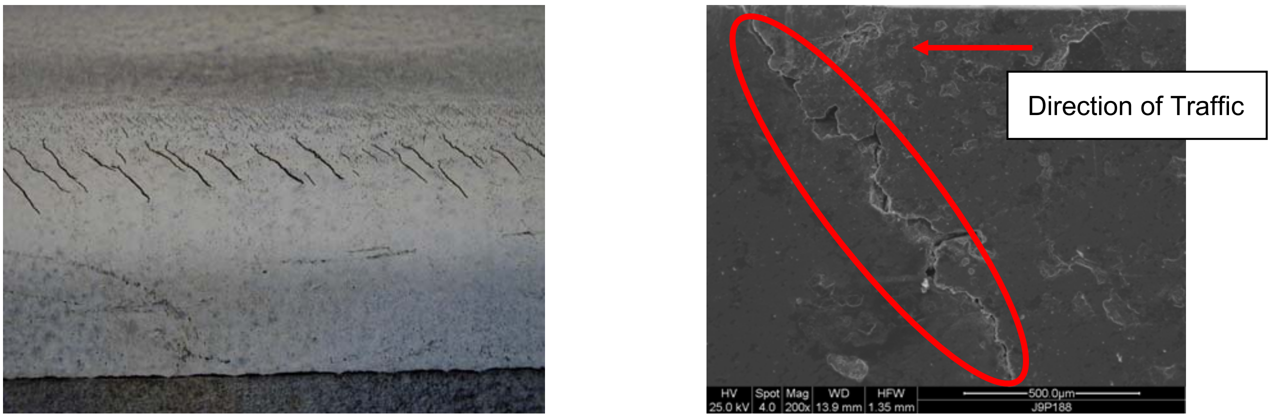

Figure 4a S3 (Lamington NR); Grade 220, 110 MGT; Moderate RCF

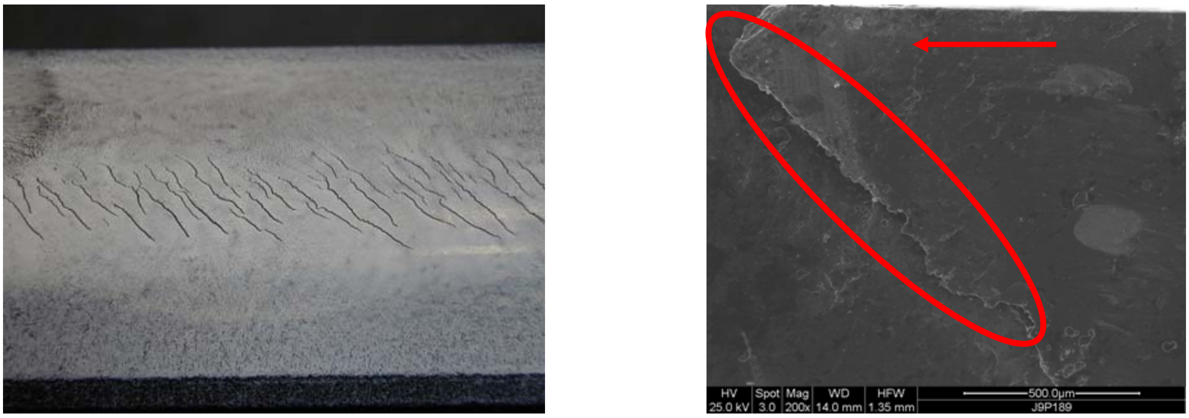

Figure 4b S4 (Lamington NR); Grade 220, 110 MGT; Heavy RCF

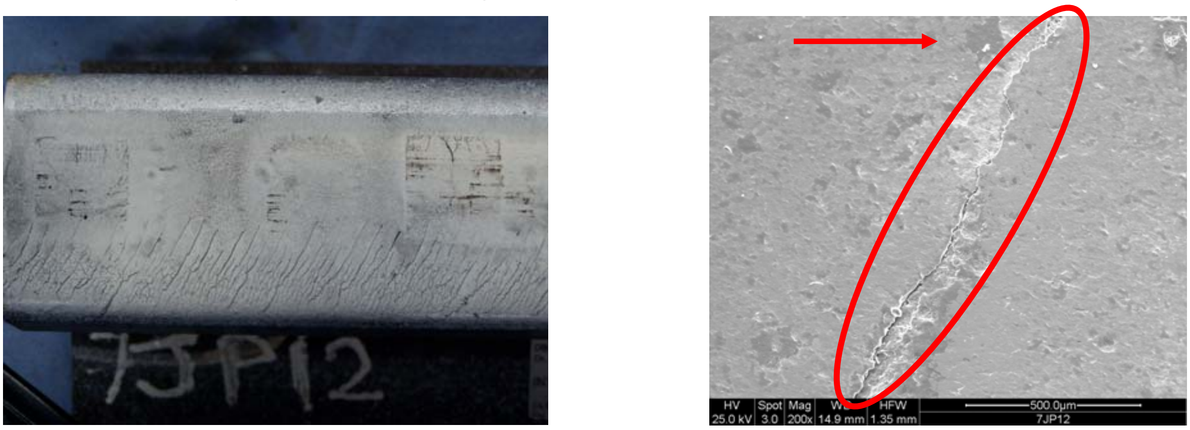

Figure 4c S9; Grade 260 (DB), 200 MGT; Severe RCF

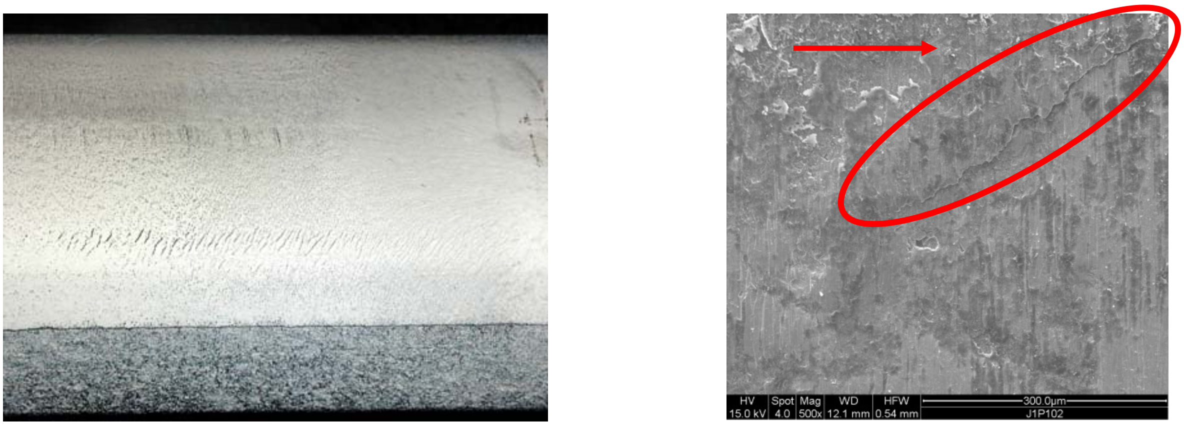

Figure 4d S11; Grade 350HT (South Side, NR), 114 MGT; Light RCF

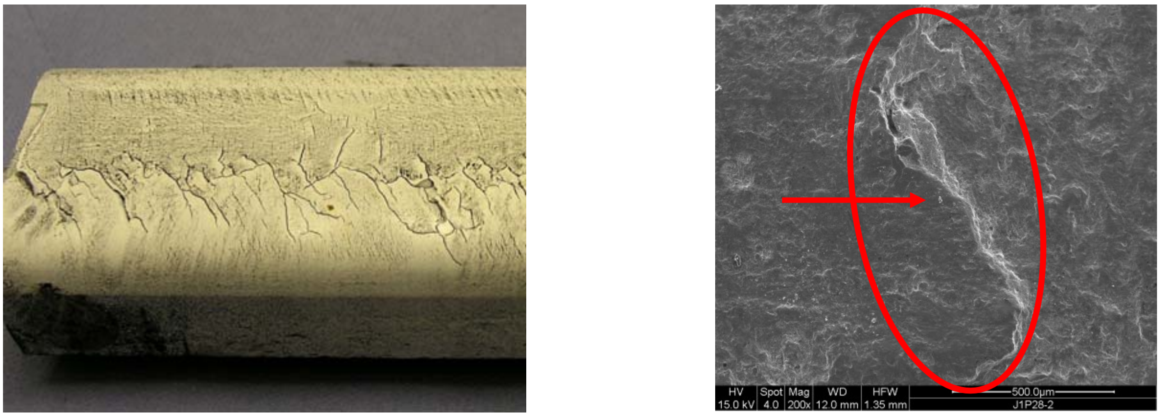

Figure 4e S12; Grade 350HT (Hatfield, NR), 78 MGT; Severe RCF

Figure 4 Rail Running Surface Examination

The following salient points are apparent from the above examination of the running surfaces of the selected matrix of samples.

1. The integrity of the rail and safety of the network is governed largely by the internal development of the crack, in particular the vertical depth. However it is difficult to measure this parameter in track and hence a need to establish a relationship with the readily visible parameter such as Surface Crack Length (SCL). Such a relationship is shown in Figure 5 and, although based on a relatively low number of samples included in this programme, it is very encouraging. It should also be noted that the regression line representing NR samples contains both Grade 220 and 350HT samples while that from the DB network is only for Grade 260 samples. Furthermore the NR and Hex samples are 56E1 while the DB are 54E3. There are only single results from the slab track network and Grade 400HB. It is hoped that further data will be generated for the final report, which may provide explanations for the observed difference.

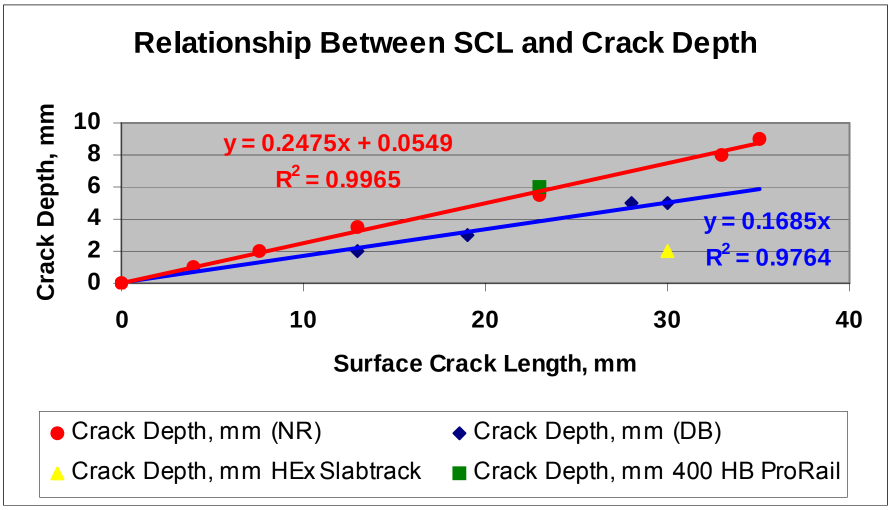

Figure 5 Relationship Between SCL and Crack Depth

2. The higher depth of focus available with Scanning Electron Microscopy has clearly revealed the formation of ledges as a result of the plastic deformation of a very thin layer of material. The magnitude of this plastic deformation appears less pronounced in the harder grades of steel. The formation of such ledges is thought to represent the origin of RCF cracks but further examination of trafficked but clear samples is necessary to establish this belief. It has been shown that such examination can be conducted on specialist replicas taken from rails in track and thereby eliminating the need to remove samples from track. (Corus internal report Dr W.T. Chao: Replication Materials for Investigation Fatigue Cracks of Rail Head).

4.3 Electron Back Scatter Diffraction Analysis

The microstructural deformation that occurs with the passage of traffic is apparent from the two micrographs of non-trafficked and trafficked sections shown in Figure 6. The significant plastic deformation of the g rains even in the presence of light category RCF is apparent.

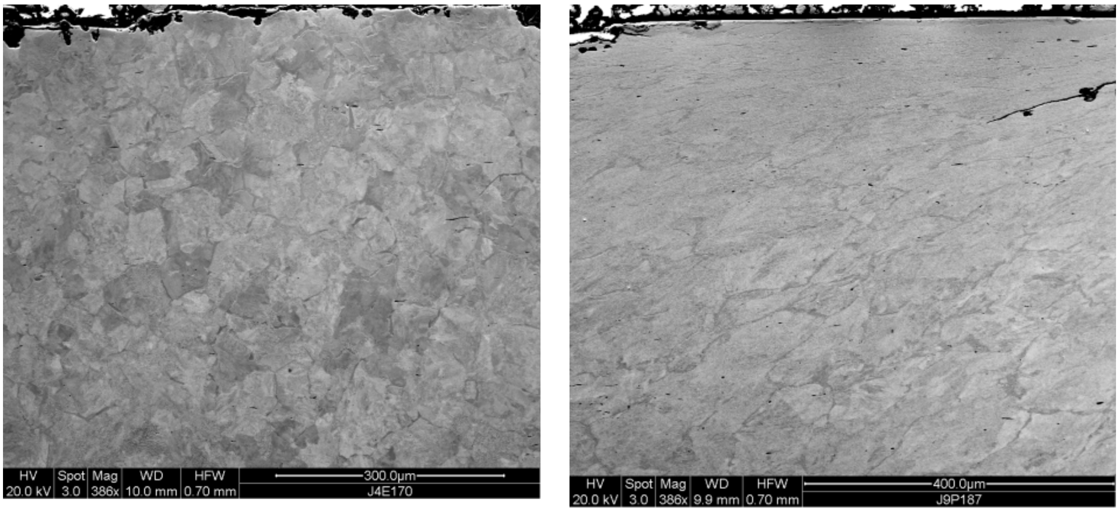

Unused rail **Light RCF cracks**

Figure 6 Showing degradation to microstructure

Traditionally, micro hardne ss ind entations have be en employed to cha racterise the strain hardening that results from the di stortion of the microstructure a nd an example of the results from thi s t echnique o n a sample after 616 MGT of traffic (Sample 5) is shown in Figure 7 below. It is apparent that the original parent rail hardness is reached at a depth of ~0.8mm and thereby suggesting little or no microstructural deformation beyond this depth. This result doe s n ot agree with the more rig orous evaluation of pl astic deformation of grains through the use of the EBSD technique, see section 4.3.1.

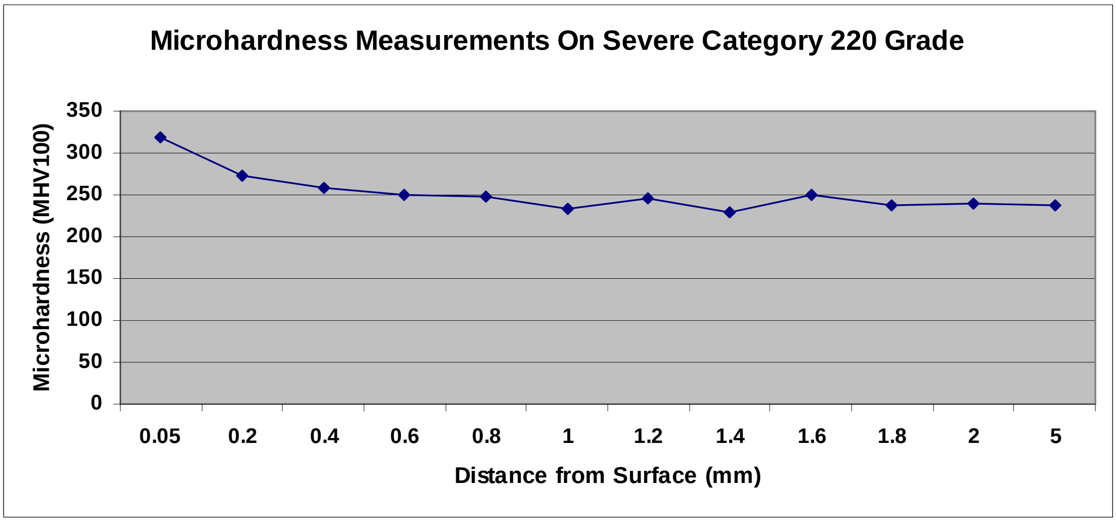

Figure 7 Determining Deformation of Microstructure from Hardness Measurements

4.3.1 EBSD Methodology

Longitudinal sections were cut through the RCF cracks close to the position of initiation on the running surface and carefully prepared for metallographic and EBSD examination. EBSD data were collected from two areas at six depths from the sample surface. Each area was 160µm x 80 µm with a 1µm step length. The depths from the surface were 0.1mm, 0.2mm, 0.5mm, 1.0mm, 2.0mm, 4.0mm and 5.0mm.

Initially, an attempt was made to use the average EBSD pattern quality from each area to show the amount of deformation within the microstructure. EBSD theory suggests that the best quality patterns are obtained from a strain free lattice and any lattice strain present will lead to a degradation of the EBSD pattern quality. For each analysis point within an area it is possible to obtain a value for the quality of the corresponding EBSD pattern image. The values obtained in this manner are then translated to get the average pattern quality for an entire area. If, due to microstructural deformation, the lattice strain is higher near to the surface and decreases with increasing depth, then pattern quality at the surface will be lower relative to that seen at depth as is apparent from Figure 8.

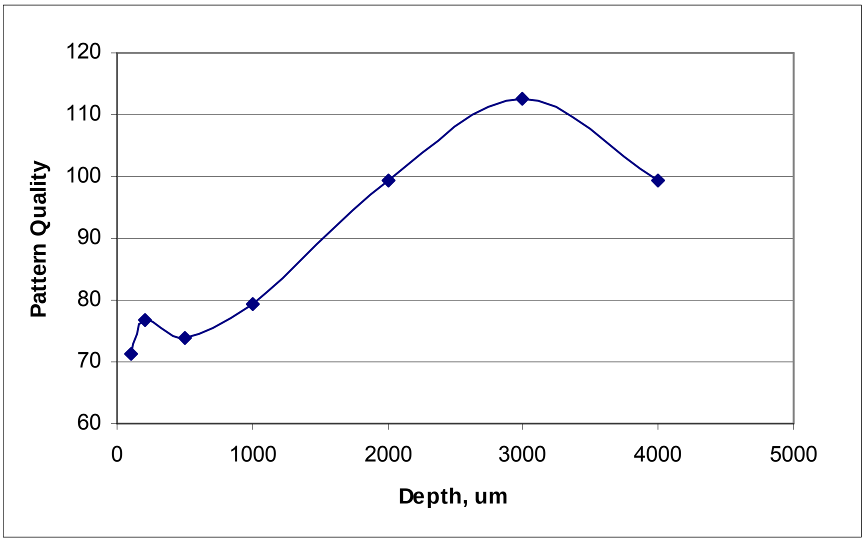

Figure 8 – Average Pattern Quality for Sample 5
(NR, Grade 220, Severe RCF)

However, the above method is not considered to be sufficiently robust because many instrumental factors can affect the quality of an EBSD pattern. Furthermore, the above technique can only be used to make valid comparisons between areas within a single sample and not between samples, again due to small instrumental variations introduced during the sample change procedure. Consequently, it was necessary to establish a parameter that is insensitive to instrumental variations.

'Kernel Average Misorientation' (KAM) maps colour code the EBSD data according to the average misorientation between a point and its neighbours. Figure 9 illustrates this calculation for a standard hexagonal grid system. A hexagonal (or square) grid does not mean the shape of the scan area is hexagonal (or square) in fact scan areas are rectangular; but rather, the individual points making up the scan area are situated on a hexagonal (or square) array. The default is the hexagonal grid, this grid is preferred over the square grid as each point in the grid has 6 equidistant neighbours; whereas, a square grid has a set of 4 neighbours to the left, right, below and above and a second set of 4 neighbours at the corners. These two sets of neighbours are not equidistant leading to a poorer description of grain boundaries in the later mapping of the data.

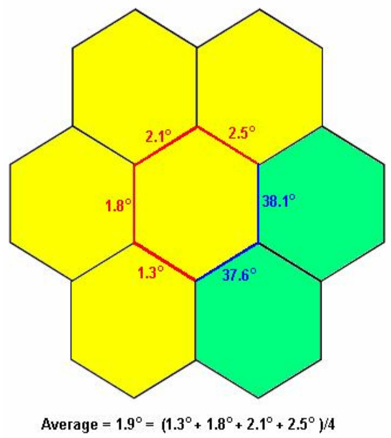

Figure 9 – Example of Kernel Average Misorientation (KAM) Calculation

The 'Maximum Misorientation' value for this exampl e is set at 3 0° so that any misorientations greater than this are omitted from the calculation. If, as in the results presented later, the maximum misorientation value is increased to the maximum allowed for iron of ~65°, the average value observed for the example in Figure 9 increases to 13.9°. The maximum value constitutes the somewhat arbitrary limit of a grai n boundary, as opposed to a range of orientations within a given grain.

The main advantage of using this approach is that the misorientation calculation is performed on orientation measurements that are not affected by the small variations in instrumental parameters that affect the pattern quality approach.

The ab ove tech nique ha s be en a pplied to all the sampl es within the mat rix in Table 1 and the results presented and discussed below. It s hould be noted that an unused rail of each Grade was analysed in a similar manner to provide a control benchmark.

4.3.1.1 EBSD Results for Grade 220

A total of five sa mples pl us a control sample were examine d from Grade 2 20 an d the Kernel Ave rage Misorientation plots are presented in Figure 10 below.

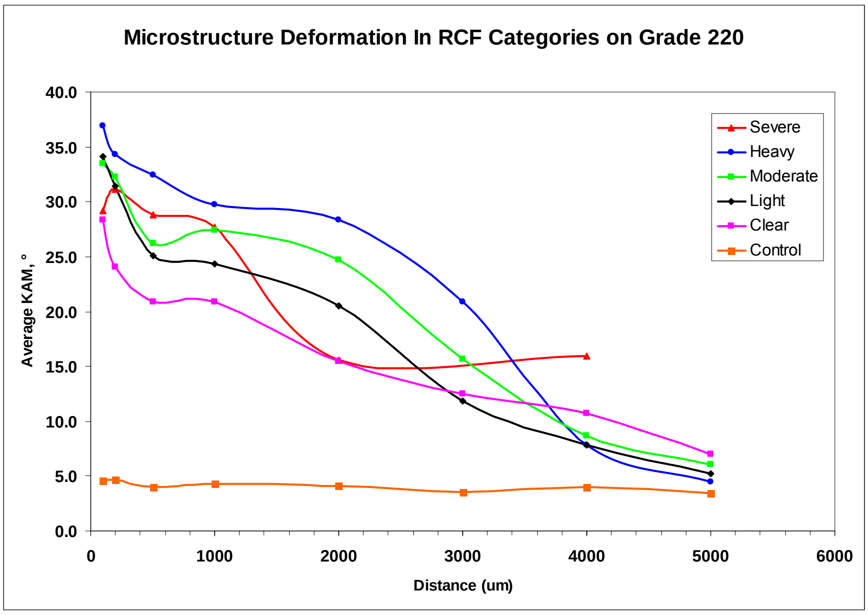

Figure 10 EBSD results for Grade 220 Samples

All samples, irrespective of the severity of the RCF cracks, show the general trend of a higher level of misorientation at the running surface that decreases gradually with depth until it reaches approximately the level exhibited by the unused control sample at a depth of 5mm.

It is also interesting to note that the level of misorientation increases with increasing length of RCF cracks except in the case of the samples within the severe category which, however, appears to have experienced microstructural deformation to a greater depth. It should be noted that the sample with the severe category of RCF cracks has experienced over 600 MGT of traffic over 30 years and its rail profile shown in Figure 1e suggests significant plastic deformation of the gauge corner and side of the head. In comparison, the samples for the light, moderate, and heavy RCF categories are from the same line and contained within a short length of track and hence have experienced the same traffic.

4.3.1.2 EBSD Results for Grade 260

A total of 4 samples covering the four categories of RCF cracks have been examined using the EBSD techniques and their KAM plots are shown in Figure 11 together with that for a control unused rail sample.

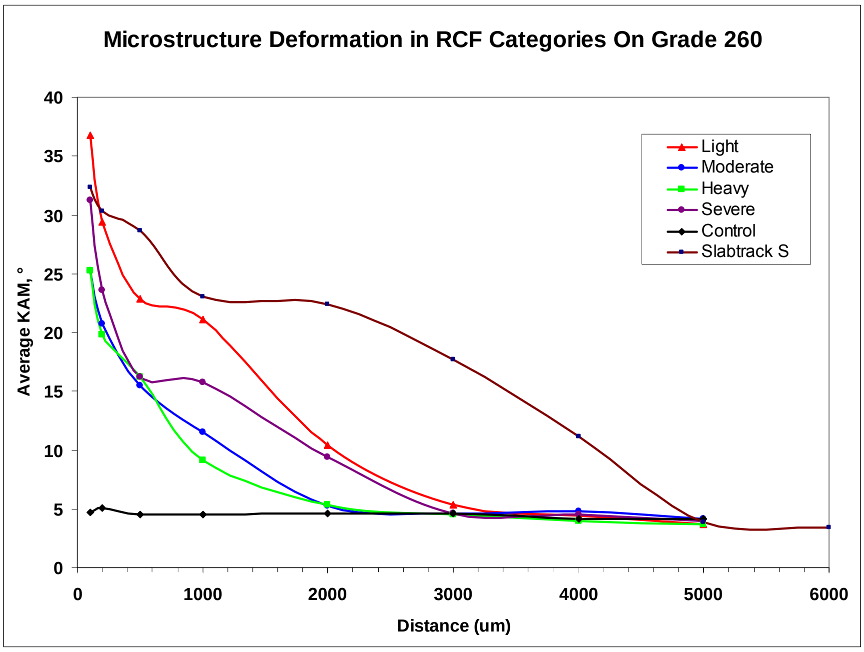

Figure 11 EBSD results for Grade 260

As in the case of Grade 220, the unused control sample exhibits very low levels of misorientation at all depths examined. The samples from the ballasted track show similar trends to the Grade 220 having higher angles of misorientation near the running surface and decreasing into the railhead to the value of the control sample at depths of 3mm. However, there does not appear to be any correlation between the levels of the average KAM value and the RCF category of the sample with the light RCF sample exhibiting higher levels of misorientation than that for the severe. Assuming that the samples are from the same curve, this observed difference is surprising and is likely to be attributable to localised contact conditions. It is necessary to establish the sample locations and any associated history to clarify the observed higher level of misorientation in the light RCF sample compared to that in Severe RCF sample.

The behaviour of the Grade 260 rail from a slab track (single vehicle track) is distinctly different from the same Grade samples from ballasted track but is similar to the Grade 220 samples from ballasted track with the average KAM value matching the control sample at a depth of 5mm. However, since only one sample has been examined from slab track configuration, it is necessary to examine further samples before any meaningful conclusions can be drawn.

4.3.1.3 EBSD Results for Grade 350HT & 400 HB

A total of 4 samples and two control samples have been examined from the two premium steel grades of 350HT and 400HB and cover the extremes of RCF categories. The plots of average KAM against depth into the head are shown in Figure 12 together with control samples for each of the two rail grades.

As before, the control samples of both premium grades show low values of misorientation at all depths examined.

The Grade 350HT sample with light RCF shows a higher level of misorientation at the surface but it decreases rapidly to the bulk level at a depth of around 1.5mm. In comparison, the Grade 350HT sample with severe RCF cracks has only a slightly increased value of the KAM close to the surface, which deceases rapidly to the bulk value. However, the in-service history of this rail is documented and it is known that it was ground a short while before it was taken out of track and the exacerbated spalling that resulted from this grinding operation will also have removed the top surface layers where the grain misorientation was the maximum.

The two samples of Grade 400HB, both with heavy RCF, depict very low KAM values that are similar to the control sample at both the rail surfaces and into the rail head. Again this sample was also ground in service, which will have lowered the observed grain misorientation which was already very limited because of the high hardness and very fine Pearlitic microstructure of this rail.

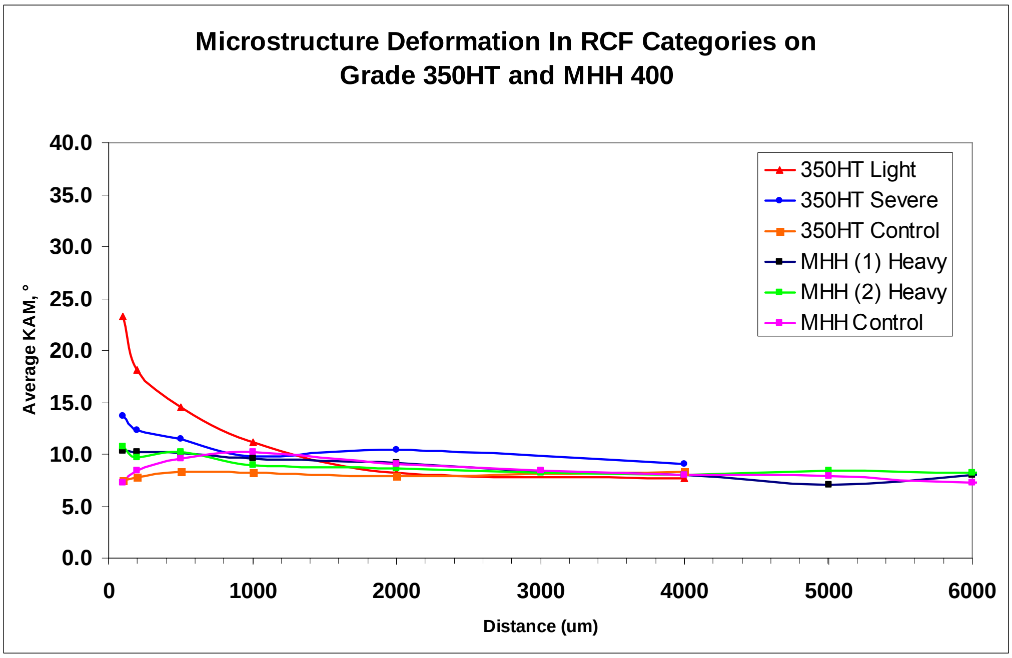

Fig 12 EBSD results for Grade 350HT and MHH 400

4.3.2 Comparison of EBSD Data for All Grades

Since the hot rolling process that is responsible for the development of the microstructure is similar for both Grades 220 and 260 (despite different manufacturers), it is not surprising that the Average KAM values are almost identical for the two control samples. In contrast the heat treated control samples reveal slightly higher values of KAM reflecting the effect of their high hardness, which is likely to concentrate the deformation in the surface layers during roller straightening.

The key finding that gives credence to the ability of this technique to provide a measure of microstructural deformation is that the KAM values in the unused control samples of all grades remain consistent to the full depths examined. The recrystallisation and the relatively high temperature transformation to a pearlitic microstructure are expected to give a uniform and low strain structure. Thus having verified the technique in this manner, its use for assessing the magnitude of "microstructural damage" from the passage of traffic and the development of RCF cracks is considered justified.

The shapes of the KAM plots show some variation particularly with respect to the severity of the RCF cracks present. The potential sliding of the crack faces against each other would be expected to increase the grain misorientation in the vicinity of the cracks. This aspect and the presence of a plateau in a number of the KAM plots of Grades 220 and 260 steels are of significant academic research interest and require further investigation. It is anticipated that the final report of this deliverable will discuss this aspect further following more detailed examination of the data and additional experimentation.

The behaviour of the Grade 260 steel from a slab track installation is significantly different to that of the behaviour of the same grade in ballasted track but resembles that observed in Grade 220 steel. Although this observation is noted, it is unrealistic to draw conclusions from a single sample and further samples with a range of RCF crack lengths need to be examined.

Finally, the most important finding of this work is the determination of the depth at which the grain misorientation in trafficked samples reaches that of unused rail i.e. the depth of the damaged layer. The values for the various grades are:

Rail Grade	Maximum Depth of "Damaged Layer"
220 >5mm	(ballasted track)
260	2.5 – 3.5mm (ballasted track)
350HT	2 – 3mm (ballasted track)
400HB <1mm	(ballasted track)

Clearly, the depth of the damaged layer is likely to have implications for the amount of metal that may need to be removed during grinding. Although only a limited number of samples have been examined in this study, the validity of the technique has been demonstrated and a more comprehensive and controlled study should be undertaken to understand the implications for grinding.

5. Interim Conclusions and Recommendations

1. The absolute measurement of vertical depths of RCF cracks in track remains a challenge for track inspection technology since current eddy current type devices are limited to relatively shallow depths. In some instances, the accuracy is limited to ~3mm depths and the decisions based on this technology may lead to premature removal of rail. Consequently, a reliable relationship between surface crack length and vertical depth of RCF cracks is a desirable solution until an alternative non-destructive inspection technique becomes available. Although based on a relatively low number of samples included in this programme, the high correlation found between SCL and vertical depth is very encouraging.
2. The higher depth of focus available with Scanning Electron Microscopy has clearly revealed the formation of ledges as a result of the plastic deformation of a very thin layer of material. The magnitude of this plastic deformation appears less pronounced in the harder grades of steel. The formation of such ledges is thought to represent the origin of RCF cracks but further examination of trafficked but clear samples is necessary to establish this belief. It has been shown that such examination can be conducted on specialist replicas taken from rails in track and thereby eliminating the need to remove samples from track.
3. Using control samples of unused rail, it has been shown that the degree of misorientation measured by EBSD technique is minimal from the surface to the measured maximum depth of 5mm as would be expected from a hot rolled and naturally transformed Pearlitic microstructure. Consequently, EBSD analysis is considered to be a credible technique to determine the magnitude of grain misorientation which can then be used as a measure of microstructural damage and its use for assessing the magnitude of "microstructural damage" from the passage of traffic and the development of RCF cracks is considered justified.
4. The behaviour of the Grade 260 steel from a slab track installation is significantly different to that of the behaviour of the same grade in ballasted track but resembles that observed in Grade 220 steel. Although this observation is noted, it is unrealistic to draw conclusion from a single sample and further samples with a range of RCF crack lengths need to be examined.
5. Finally, the most important finding of this work is the determination of the depth at which the grain misorientation in trafficked samples reaches that of unused rail i.e. the depth of the damaged layer. The values indicate a decreasing depth of damaged layer with increasing hardness of the rail. Clearly, the depth of the damaged layer is likely to have implications for the amount of metal that may need to be removed during grinding. Although only a limited number of samples have been examined in this study, the validity of the technique has been demonstrated and a more controlled study is required to answer the following fundamental questions:
    1. Does the full depth of damaged layer need to be removed during grinding?
    2. Is the period to initiation of RCF cracks more rapid following grinding if the full depth of damaged layer is not removed?
    3. Is the probability of sub-surface initiation of RCF cracks increased if the full depth of damaged layer is not removed?
    4. Does the very limited depth of "damaged layer" in the high hardness grade allow small amounts of metal to be removed during grinding to expose undamaged material and start a new life cycle and thereby increase life of rails.

It is evident that further work is necessary to answer the above questions and such a programme requires close collaboration between Infrastructure Managers, grinding service providers, the rail manufacturers, and research organisations capable of undertaking EBSD analysis. The current document provides a basis for discussion, particularly within SP4 partners of Innotrack, to establish the details of such a programme.

6. Background References

1. Black M. an d Hig ginson R.L. (1 999), 'An Invest igation into the Use of Ele ctron Ba ck S cattered Diffraction to Measure Recrystallised Fraction', Scripta Materialia, Vol.41, No.2 pp 125-129.

2. Farooq M.U., "Electron Back-Scattered Diffraction on Anisotropic Steels", Diploma Thesis, Chalmers University of Technology, widen 2001.

3. Floer, W., Hu, Y.M., Kr upp, U., Chri st H.-J.: Application of the EBSD Technique to Study the Initiation and Propa gation of Short Cra cks, Pra ktische Metallo graphie – P ractical Metallo graphy, 7 (2002)

4. Gourgues, A. –F. (2001), 'Electron backscatter diff raction an d cra cking', M aterials Scie nce a nd Technology, vol.18, pp 119.

5. Juul Jensen, D. (20 00) 'Three-dimensional Ori entation Imaging'. Chapter 8 in E lectron Ba ckscatter diffraction in Materials Science. Eds. A.J. Schwartz et al. Plenum Publishers, New York, 91-104.

6. Lloyd, G.E., Farmer, A.B. and Mainp rice, D. (1 997) 'Misori entation analy sis a nd the format ion and orientation of subgrain and grain boundaries'. Tectonophysics 279, 55-78.

7. Randle, V., (2000) 'Fundamental aspects of ele ctron back-scatter diffraction, in Automated Electron Backscatter Diffractio n'. Ed. A. Schwartz, M. Ku mar a nd B. Adams, Klu wer A cademic/Plenum Publishers, New York, 19-30.

8. Schwarzer, R.A., (1997) 'A utomated crystal lattice orientation ma pping u sing a computer-controlled SEM'. Micron 28, 249-265.

9. Schwarzer, R.A. (2000) 'Automated electron backscatter diffraction: present state and prospects'. In: A.J. Sch wartz, M. Kuma r and B.L. A dams (e ds.): Electron b ackscatter diffraction in materials science. Kluwer Academic/Plenum Press New York, pp. 105-122.

10. Wilkinson, A.J. 'Mea suring Strain s u sing Electr on B ack Scatter Diffraction' in "Elec tron Bac kscatter Diffraction in Materi als S cience" eds. Adam s B. L., Schwarz A. J. an d Kumar M., (Kluwe r Academic/Plenum Publishers).